JOURNAL OF SOLID STATE CHEMISTRY 25, 121–135 (1978)

Vibrational Spectra and Force Constants of Rare Earth and Scandium Thiospinels*

STEVEN I. BOLDISH AND WILLIAM B. WHITE†

Materials Research Laboratory, The Pennsylvania State University, University Park, Pennsylvania 16802

Received September 9, 1977; in revised form, December 21, 1977.

Infrared and Raman spectra were measured for AB_2S_4 spinels (A = Cd, Mg, or Zn; B = Sc, Yb, or Tm). The four T_{1u} ir bands and four of the five ($A_{1g} + E_g + 3T_{2g}$) Raman bands were generally observed. Symmetry coordinates were calculated for the spinel structure and normal coordinates were calculated using a model containing four force constants. Good fits of the eight observed vibrational frequencies were obtained from four force constants. The tetrahedral stretching constants have values between 1.41 and 0.49 mdyn/Å, while the octahedral stretching constants have values between 0.61 and 0.38 mdyn/Å. The tetrahedral stretching constant was always larger for Cd compounds than for compounds containing the smaller Mg ion in tetrahedral sites, suggesting a measure of the additional stabilization of Cd through covalent bonding. Calculated absorbances for the ir transverse mode frequencies were in reasonable agreement with experiment and support the four-force-constant model.

Introduction

In the past few years there has been an increasing interest in the sulfide and selenide spinels. Examples of these compounds which give good Raman spectra are not very numerous, since most have a metallic luster. However, infrared spectra of the powdered compounds are easily obtained. This paper is concerned with the vibrational properties of some *RE* and Sc sulfide spinels with the general formula AB_2S_4, where A = Cd, Mg, or Zn, and B = Yb, Tm, or Sc. It is our intention to study the relationship of the vibrational spectra of these compounds to their structure and composition. The data were obtained from powders and the compounds were studied as a family.

* Research supported by the Air Force Cambridge Research Laboratories under Contract F19628-71-C-0232 and by the National Science Foundation under Grant EAR 73-00243 A01.

† Also affiliated with the Department of Geosciences.

Most previous work concerns the oxide spinels and numerous papers have been written relating the number and positions of bands in the ir spectra to structure and composition. Preudhomme and Tarte in an important series of papers review most of the earlier work (*1–4*).

Articles discussing sulfide and selenide spinels are primarily concerned with single-crystal ir or Raman measurements of just a few compounds. However, the powder ir spectra of some 14 sulfide spinels have been reported by Lutz and Feher (*5*). Single-crystal specular reflectance measurements have been made on $CdIn_2S_4$ (*6*, *7*), $CdCr_2Se_4$ (*8*, *9*), $CdCr_2S_4$ (*8*), and $HgCr_2Se_4$ (*10*). Single-crystal polarized Raman measurements have been made on $CdIn_2S_4$ (*11*, *12*), $CdCr_2S_4$ (*12*, *13*), and $CdCr_2Se_4$ (*13*).

Compounds with the spinel structure have the general formula AB_2X_4 (X is either O, S, or Se) with space group $Fd3m(O_h^7)$. There are

0022–4596/78/0252–0121$02.00/0

TABLE I

LATTICE PARAMETERS FOR SULFIDE SPINELS

Compound	Measured lattice parameter a_0 (Å)	Literature values of lattice parameters		References
		u	a_0 (Å)	
$MgTm_2S_4$	10.98	—	10.958	(*20*)
$MgYb_2S_4$	10.95	0.377	10.957	(*21*)
$MgSc_2S_4$	10.62	0.383	10.627	(*21*)
$ZnSc_2S_4$	10.48	—	10.483	(*20*)
$CdTm_2S_4$	11.10	0.257?	11.09(2)	(*22*)
$CdYb_2S_4$	11.07	0.382	11.0684	(*22*)
$CdSc_2S_4$	10.73	—	10.733	(*22*)

eight formula units in the face-centered cell. The 56 atoms in this cell occupy the following positions: A, $8a(T_d)$; B, $16d(D_{3d})$; and X, $32e(C_{3v})$. Only the primitive unit cell is necessary for a vibrational analysis. There are several ways of choosing this cell, but it is of no consequence because the vibrational analysis yields identical results for any of the choices. A factor group analysis of the spinel structure (*14*) predicts the vibrational modes

$$\Gamma = (A_{1g} + E_g + 3T_{2g})(\text{Raman active}) + 4T_{1u}(\text{ir active}) + (T_{1g} + 2A_{2u} + 2E_u + 2T_{2u})(\text{inactive}).$$

Force constant calculations that have been used for spinel compounds are for the most part very simple and employ modified *FG* matrix calculations (*15–18*). On the other hand there has been a rigorous treatment of the lattice dynamics of one spinel $MgAl_2O_4$ (*19*) which used a rigid ion approximation.

It is with the Brüesch and D'Ambrogio model (*17*) that our infrared and Raman data are analyzed. This model is applicable because the assumptions made in its formulation hold true for these covalent sulfides with short-range forces.

Experimental

The spinels were prepared by sulfurizing the sesquioxides and then reacting the sesquisulfides with the sulfides of the divalent metal. It was necessary to use H_2S as the sulfurizing agent. H_2S reacts with the *RE* sesquioxides at temperatures above 1200°C. The reaction system consisted of a graphite susceptor, containing the oxide, which was RF heated in an H_2S atmosphere. Samples could be heated to above 1300°C and converted to the sesquisulfides within half an hour using this technique. The subsequent formation of the spinels was accomplished by mixing the sesquisulfides with appropriate amounts of CdS, MgS, or ZnS. The mixtures were then fired at 1200°C in evacuated silica tubes. The spinels thus formed were characterized by X-ray powder diffraction and precise lattice parameters were obtained (Table I).

Infrared spectra of selected spinels were measured from 33 to 800 cm^{-1} on powders dispersed in Nujol and spread on polyethylene plates. The measurements were made using a Beckman IR-11 spectrophotometer in double-beam operation.

While ionic materials frequently give meaningless powder ir spectra, the more covalent sulfide spinels seem to give reasonably accurate powder transmission spectra. The validity of using powder techniques is demonstrated with data for $CdIn_2S_4$. Both reflectance (*6*) and powder transmission data (*5*) are available for comparison. Table II presents the literature results of far-infrared powder transmission and reflectance measurements. In addition values of υ_c, the frequencies of the reflectance band maxima, are tabulated as measured from the single-crystal reflectance spectrum. The separation of the transverse and

longitudinal modes of $CdIn_2S_4$ is of the order of 1–2 cm^{-1} for the sharp bands and 32 and 55 cm^{-1} for the intense broad bands. The reflectance band with the largest longitudinal optic–transverse optic splitting yields the transverse mode whose frequency differs the most from its position in the powder spectrum. This same reflectance band also has the highest oscillator strength so that it should give a transmission band in the powder spectrum which has considerable reflectance character. That the band in the powder spectrum is reflectance-like is indicated by comparing υ_c to the mode frequency υ_t in the powder spectrum. υ_c is 230 cm^{-1} while υ_t is 231 cm^{-1}.

Raman measurements were made using a Spex Ramalog Double Monochromator-Spectrometer with an RCA C31034 photomultiplier detector with photon counting electronics and an excitation source of either a Spectra Physics Model 164 Ar^+ laser or a Model 124A He–Ne laser. Measurements were made on pressed pellets of the sulfides and the power of the laser beam was kept at a minimum to avoid damage to the surface of the pellet. The final measurements were made with the 15-mW 632.8-nm He–Ne laser.

Spectra

Infrared spectra of the thiospinels examined are shown in Figs. 1 and 2; the Raman spectra are shown in Figs. 3 and 4. The measured fundamental frequencies are compiled in Table III.

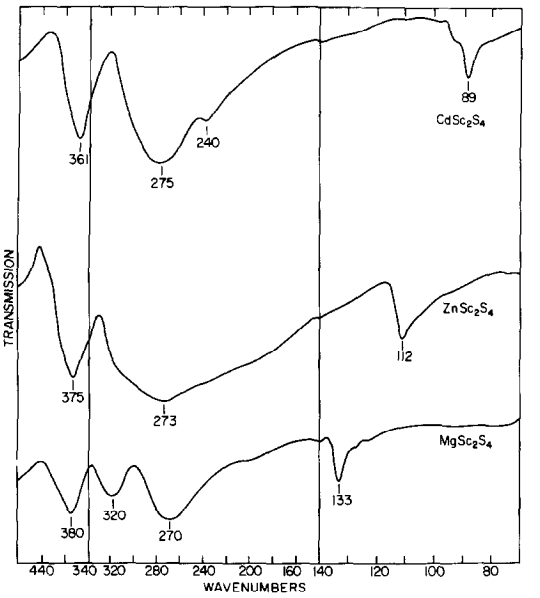

FIG. 1. Infrared spectra of the ASc_2S_4 spinels (A = Cd, Zn, Mg).

The infrared spectra are typical of spinel compounds. There are two very intense broad bands and two weaker bands. Sometimes one or both of the weaker bands are not observed. X-Ray data confirm that the compounds studied are normal spinels, so that the spectra observed arise from the cation configuration given previously.

The Raman spectra shown in Figs. 3 and 4 were measured with a He–Ne laser. There should be five Raman-active modes. Only four fundamental bands are observed consistently

TABLE II

COMPARISON OF TRANSVERSE MODE POSITIONS FOR $CdIn_2S_4$ FROM POWDER TRANSMISSION AND SINGLE-CRYSTAL REFLECTANCE[a]

	υ_6	υ_7	υ_8	υ_9
Powder transmission (5)				
υ_t (cm^{-1})	311	231	170	68
Reflectance (6)				
υ_t (cm^{-1})	307	215	171	68
υ_c (cm^{-1})	320	230	170	68
υ_l (cm^{-1})	339	270	172	69
$4\pi\rho$	0.63	5.20	0.5	0.3
γ	0.021	0.020	0.040	0.040

[a] υ_c is equal to the frequency of a reflectance band maximum.

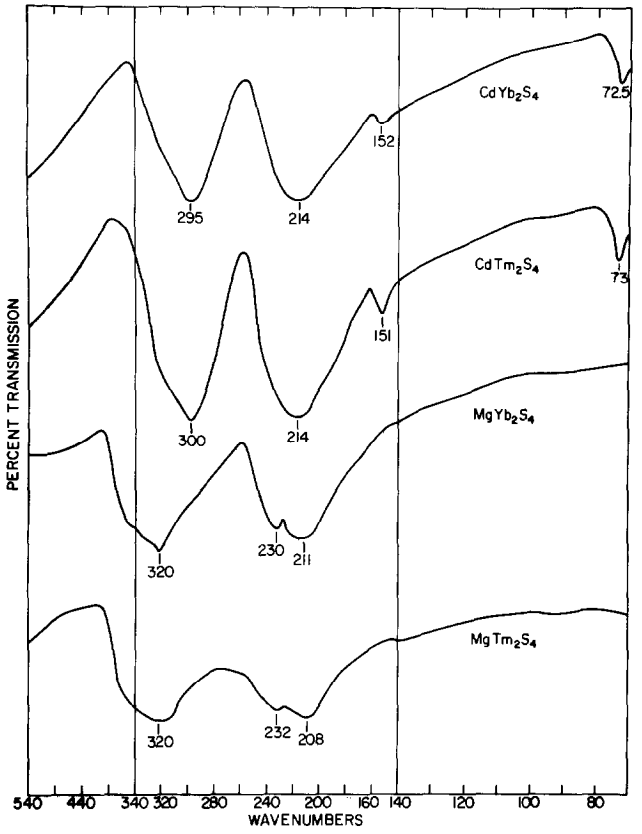

FIG. 2. Infrared spectra of the ARE_2S_4 spinels (A = Mg, Cd; RE = Yb, Tm).

in the spectra of most of the compounds. A fifth band appears only in the spectra of $ZnSc_2S_4$ and $MgSc_2S_4$, but it is unclear at this point if this fifth band is the missing fundamental mode.

The Raman spectra of the cadmium spinels excited by the argon laser contain more lines than permitted by group theory. The extra bands are very strong and dominate the spectra of the Cd spinels, while the fundamental bands are very weak by comparison. In the spectrum of $CdYb_2S_4$ the extra bands form a progression and occur at 300, 600, and 915 cm^{-1} with decreasing intensity. In the spectrum of $CdTm_2S_4$ a strong band occurs at 301 cm^{-1} with an apparently related band at 602 cm^{-1} and again the intensities decrease with increasing frequency. Now, however, there are other weaker bands situated around the 602-cm^{-1} band. While the nonfundamental bands dominate the $CdYb_2S_4$ spectrum, they are minor features in the $CdTm_2S_4$ spectrum. In the spectrum of $CdSc_2S_4$ a whole new group of bands appears. Here a progression seems to be formed by the 308-, 395-, and 485-cm^{-1} bands with a spacing of ~88 cm^{-1}, but the change in intensity is irregular. There is still the same progression formed by the 308- and the 602-cm^{-1} bands found in the other Cd compounds.

The extra features in these spectra appear to be due to multiphonon processes in traces of free CdS which have been enhanced by a resonance effect. Bands at regular intervals have been found in the resonance Raman spectra of single crystals of CdS at nearly the same positions as for these spinel compounds (*23*).

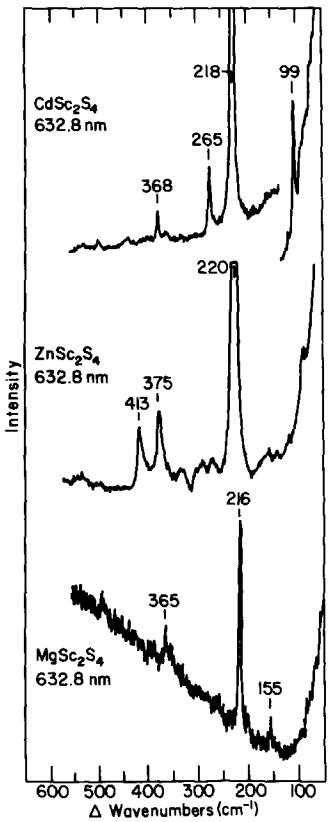

FIG. 3. Raman spectra of the ASc_2S_4 spinels. Excitation by 15-mW He–Ne Laser.

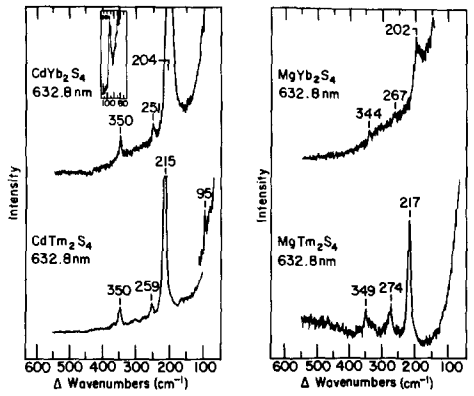

FIG. 4. Raman spectra of the ARE_2S_4 spinels. Excitation by 15-mW He–Ne laser.

Symmetry Coordinates for the Spinel Structure

The dynamical matrix used to describe the vibrational properties of crystals has dimensions $3N\sigma \times 3N\sigma$, where N is the number of atoms in a primitive unit cell and σ is the number of primitive unit cells in the crystal. The translational symmetry of the lattice factors the dynamical matrix into $\sigma - 3N \times 3N$ subblocks where each subblock is labeled by one of the σ k-vectors that can be assigned to the vibrations. The dynamical matrix for a particular k-vector can then be described using the notation of Born and Huang (*24*).

$$D_{\alpha\beta}\begin{pmatrix}\mathbf{k}\\ kk'\end{pmatrix} = \frac{1}{(m_k m_{k'})^{1/2}} \times \sum_{l'} \Phi_{\alpha\beta}\begin{pmatrix}l'\\ kk'\end{pmatrix} \exp\ [-2\pi i\mathbf{k}\cdot\mathbf{x}(l')], \quad (1)$$

$$\Phi_{\alpha\beta}\begin{pmatrix}l'\\ kk'\end{pmatrix} = \frac{\partial^2\Phi}{\partial u_\alpha\binom{0}{k}\,\partial u_\beta\binom{l'}{k'}}\Bigg)_0, \quad (2)$$

where $\alpha,\beta = x,y,z$; $k,k' = 1,2,\ldots,N$; $l' = 0,1,\ldots,\sigma$. α and β define the directions of displacement, k and k' are the labels of the primitive unit cell, and l' is a label for the different unit cells. In the above equations Φ is

TABLE III

RAMAN AND INFRARED MODES FOR THIOSPINELS

	$\upsilon_1(A_{1g})$	$\upsilon_2(E_g)$	$\upsilon_3(T_{2g})$	$\upsilon_4(T_{2g})$	$\upsilon_5(T_{2g})$	$\upsilon_6(T_{1u})$	$\upsilon_7(T_{1u})$	$\upsilon_8(T_{1u})$	$\upsilon_9(T_{1u})$
$CdSc_2S_4$	—	368	218	—	265	99	361	275	240	89
$ZnSc_2S_4$	413	375	220	—	—	—	375	273	—	112
$MgSc_2S_4$	490	365	216	—	—	155	380	270	320	133
$CdYb_2S_4$	—	350	204	—	251	96	295	214	152	72.5
$CdTm_2S_4$	—	350	215	—	259	95	300	214	151	73
$MgYb_2S_4$	—	344	202	—	267	—	320	211	230	—
$MgTm_2S_4$	—	349	217	—	274	—	320	208	232	—

the crystal potential, $\mathbf{x}(l')$ is a lattice vector which connects unit cells l' and the 0. m_k and $m_{k'}$ are the masses of atoms k and k', and $u_\alpha(l'_k)$ is the displacement of atom k of the l'th unit cell in the α direction. $\Phi_{\alpha\beta}(l'_{kk'})$ is just the negative of the force on atom k in the zeroth unit cell in the α direction due to a unit displacement of atom k' in the l' cell in the β direction. However, these general expressions can be simplified if one is interested in first-order ir absorption and Raman scattering where $\mathbf{k} \cong 0$.

The dynamical matrix describing the optically active vibrations at $\mathbf{k} \cong 0$ is

$$D_{\alpha\beta}\begin{pmatrix}0\\kk'\end{pmatrix} = \frac{1}{(m_k m_{k'})^{1/2}} \sum_{l'} \Phi_{\alpha\beta}\begin{pmatrix}l'\\kk'\end{pmatrix}. \quad (3)$$

The determinant of the dynamical matrix must equal zero if nontrivial solutions to the vibrational secular equations exist. Thus

$$|D_{\alpha\beta}(^0_{kk'}) - \omega^2 \delta_{\alpha\beta}\delta_{kk'}| = 0, \qquad \omega^2 = 4\pi^2 c^2 \upsilon^2; \quad (4)$$

υ is in units of cm^{-1}. If D is the dynamical matrix and E is a unit matrix then the above equation can be written as $|D - \omega^2 E| = 0$.

The Wilson FG matrix formalism as extended to crystals by Shimanouchi *et al.* (*25*) has the same form as the dynamical matrix: $|FG - \omega^2 E| = 0$, $D \equiv FG$. Here F is a matrix dependent on the force field and G is a matrix dependent on the structure of the crystalline solid and the masses of the constituent atoms. Brüesch and D'Ambrogio (*17*) used this formalism for calculating the dynamical matrix of sulfide and selenide spinels.

The dynamical matrix at $\mathbf{k} \cong 0$ can be factored by combining the $3N$ displacement coordinates into $3N$ orthogonal symmetry coordinates. The symmetry coordinates form basis vectors of the different irreducible representations of the point group of the crystal. The subblocks of the factored dynamical matrix are in turn completely diagonalized by the normal coordinates to yield the squares of the vibrational frequencies. The normal coordinate Q^d_{ni} belongs to the dth irreducible representation of the point group of the crystal, is g-fold degenerate, and has m distinct frequencies associated with it. Q^d_{ni} is formed by combining the symmetry coordinates S^d_{ji} according to the equation

$$Q^d_{ni} = \sum_{j=1}^{m} b^d(n, j)\, S^d_{ji}, \qquad i = 1, 2, \ldots, g,\ n = 1, 2, \ldots, m. \quad (5)$$

The quantities $b^d(n,j)$ are related to the amplitudes of vibration for the different atoms in the unit cell and are determined by the values of the force constants and the force field chosen. They are, however, uniquely determined by symmetry and are independent of the force constant when there is only one frequency in a particular irreducible representation.

The 42 symmetry coordinates for the spinel structure were derived using the Worlton–Warren computer program (*26*). Because only the zone center phonon frequencies are needed, the input into the program is just the atomic positions in the primitive unit cell, the characters of the irreducible representations of the O_h point group, and the diagonal matrix elements from all the degenerate irreducible representations.

The diagonal matrix elements for the irreducible representations were obtained by deriving the appropriate coordinate transformation matrices. These matrices were generated by forming the direct product representations of T_d and C_i, $O_h = C_i \otimes T_d$. The different matrix representations for the operations of T_d were generated using the basis functions listed in the point group character tables (*27*). The irreducible representations for the different operations of the point group C_i (E and i) are just the characters in the point group table, since the irreducible representations are all one-dimensional.

The symmetry coordinates for the Raman and ir-active modes of the spinel structure are listed in Table IV. A complete list is given in (*17*). There are a total of 42 symmetry coordinates corresponding to the $3N$ degrees

TABLE IV

SYMMETRY COORDINATES FOR THE RAMAN AND INFRARED MODES OF THE SPINEL STRUCTURES[a]

$$S_{11}^{A_{1g}} = 1/(6^{1/2}2)(x_7 + y_7 + z_7 + x_8 - y_8 - z_8 - x_9 + y_9 - z_9 - x_{10} - y_{10} + z_{10} - x_{11} - y_{11} - z_{11} - x_{12} + y_{12} + z_{12} + x_{13} - y_{13} + z_{13} + x_{14} + y_{14} - z_{14})$$

$$S_{11}^{E_g} = 1/(3^{1/2}4)(x_7 + y_7 - 2z_7 + x_8 - y_8 + 2z_8 - x_9 + y_9 + 2z_9 - x_{10} - y_{10} - 2z_{10} - x_{11} - y_{11} + 2z_{11} - x_{12} + y_{12} - 2z_{12} + x_{13} - y_{13} - 2z_{13} + x_{14} + y_{14} + 2z_{14})$$

$$S_{12}^{E_g} = 1/4(x_7 - y_7 + x_8 + y_8 - x_9 - y_9 - x_{10} + y_{10} - x_{11} + y_{11} - x_{12} - y_{12} + x_{13} + y_{13} + x_{14} - y_{14})$$

$$S_{11}^{T_{2g}} = 1/2^{1/2}(y_1 - y_2)$$

$$S_{21}^{T_{2g}} = 1/(2^{1/2}2)(y_7 + y_8 + y_9 + y_{10} - y_{11} - y_{12} - y_{13} - y_{14})$$

$$S_{31}^{T_{2g}} = 1/4(x_7 + z_7 - x_8 + z_8 - x_9 - z_9 + x_{10} - z_{10} - x_{11} - z_{11} + x_{12} - z_{12} + x_{13} + z_{13} - x_{14} + z_{14})$$

$$S_{12}^{T_{2g}} = 1/2^{1/2}(x_1 - x_2)$$

$$S_{22}^{T_{2g}} = 1/(2^{1/2}2)(x_7 + x_8 + x_9 + x_{10} - x_{11} - x_{12} - x_{13} - x_{14})$$

$$S_{32}^{T_{2g}} = 1/4(y_7 + z_7 - y_8 - z_8 - y_9 + z_9 + y_{10} - z_{10} - y_{11} - z_{11} + y_{12} + z_{12} + y_{13} - z_{13} - y_{14} + z_{14})$$

$$S_{13}^{T_{2g}} = 1/2^{1/2}(z_1 - z_2)$$

$$S_{23}^{T_{2g}} = 1/(2^{1/2}2)(z_7 + z_8 + z_9 + z_{10} - z_{11} - z_{12} - z_{13} - z_{14})$$

$$S_{33}^{T_{2g}} = 1/4(x_7 + y_7 - x_8 + y_8 + x_9 - y_9 - x_{10} - y_{10} - x_{11} - y_{11} + x_{12} - y_{12} - x_{13} + y_{13} + x_{14} + y_{14})$$

$$S_{11}^{T_{1u}} = 1/2^{1/2}(x_1 + x_2)$$

$$S_{21}^{T_{1u}} = 1/2(x_3 + x_4 + x_5 + x_6)$$

$$S_{31}^{T_{1u}} = 1/(2^{1/2}2)(y_3 + z_3 - y_4 - z_4 - y_5 + z_5 + y_6 - z_6)$$

$$S_{41}^{T_{1u}} = 1/(2^{1/2}2)(x_7 + x_8 + x_9 + x_{10} + x_{11} + x_{12} + x_{13} + x_{14})$$

$$S_{51}^{T_{1u}} = 1/4(y_7 + z_7 - y_8 - z_8 - y_9 + z_9 + y_{10} - z_{10} + y_{11} + z_{11} - y_{12} - z_{12} - y_{13} + z_{13} + y_{14} - z_{14})$$

$$S_{12}^{T_{1u}} = 1/2^{1/2}(y_1 + y_2)$$

$$S_{22}^{T_{1u}} = 1/2(y_3 + y_4 + y_5 + y_6)$$

$$S_{32}^{T_{1u}} = 1/(2^{1/2}2)(x_3 + z_3 - x_4 + z_4 - x_5 - z_5 + x_6 - z_6)$$

$$S_{42}^{T_{1u}} = 1/(2^{1/2}2)(y_7 + y_8 + y_9 + y_{10} + y_{11} + y_{12} + y_{13} + y_{14})$$

$$S_{52}^{T_{1u}} = 1/4(x_7 + z_7 - x_8 + z_8 - x_9 - z_9 + x_{10} - z_{10} + x_{11} + z_{11} - x_{12} + z_{12} - x_{13} - z_{13} + x_{14} - z_{14})$$

$$S_{13}^{T_{1u}} = 1/2^{1/2}(z_1 + z_2)$$

$$S_{23}^{T_{1u}} = 1/2(z_3 + z_4 + z_5 + z_6)$$

$$S_{33}^{T_{1u}} = 1/(2^{1/2}2)(x_3 + y_3 - x_4 + y_4 + x_5 - y_5 - x_6 - y_6)$$

$$S_{43}^{T_{1u}} = 1/(2^{1/2}2)(z_7 + z_8 + z_9 + z_{10} + z_{11} + z_{12} + z_{13} + z_{14})$$

$$S_{53}^{T_{1u}} = 1/4(x_7 + y_7 - x_8 + y_8 + x_9 - y_9 - x_{10} - y_{10} + x_{11} + y_{11} - x_{12} + y_{12} + x_{13} - y_{13} - x_{14} - y_{14})$$

[a] S_{ji}^{d} represents the symmetry coordinates where $i = 1, 2, \ldots, g$; $j = 1, 2, \ldots, m$. This symmetry coordinate is the ith member of the jth degenerate set forming a basis for the dth irreducible representation. Coordinates grouped close together in the table are those which must be combined to form normal coordinates. The components are numbered 1, 2 = tetrahedral cations; 3–6 = octahedral cations; and 7–14 = anions. Within each equipoint, the atoms are numbered in the same order as they are listed in the International Tables for Crystallography.

of freedom ($N = 14$ for spinel). The displacement coordinates x_i, y_i, and z_i are mass-weighted Cartesian coordinates and are parallel to the (100), (010), and (001) axes of the face-centered cell. The subscripts 1 and 2 label the tetrahedral ions, A; 3 to 6 label the octahedral ions, B; and 7 to 14 label the anions. The numbering scheme corresponds to the listing of equipoints given in the International Tables for Crystallography. Each symmetry

coordinate forms a 1 × 42 column vector in which most entries are zero.

When more than one mode belongs to a symmetry species, the symmetry coordinates must be combined to form normal coordinates. The coefficients used to form the combinations depend on the details of the dynamical equations. The Raman-active T_{2g} normal coordinates are a combination of three symmetry coordinates, while the infrared-active T_{1u} normal coordinates are a combination of five symmetry coordinates. However, for those symmetry species with only one mode, the normal coordinates are just equal to the symmetry coordinates. In Table IV symmetry coordinates which are to be combined to form normal coordinates are grouped together. The number of symmetry coordinates within a group is equal to the number of distinct modes predicted by the factor group. The number of groups listed with a certain symmetry is equal to the degeneracy of the symmetry species.

Mode Assignments

The Raman-active modes do not involve motions of the octahedral cations because these cations are located on the centrosymmetric 16*d* sites. The Raman modes for spinel compounds are of *g* character and must preserve the center of symmetry. The A_{1g}, E_g, and T_{2g} symmetry coordinates in Table IV have no displacement coordinates for the octahedral cations. In addition, consideration of the symmetry coordinates of the A_{1g} and E_g modes shows that these modes involve motions of only the sulfur atoms so that these frequencies are unaffected by the masses of both the octahedral and tetrahedral cations. The three T_{2g} modes are the only modes whose frequencies should be functions of the tetrahedral atom masses.

Table III shows that υ_4 and υ_5 are the modes most strongly affected by changing the tetrahedral cation mass. When the mass of the tetrahedral cation is changed from 112.4 to 24.312 amu by substituting a Mg for a Cd atom in the Sc spinels, υ_5 shifts from 99 to 155 cm^{-1}. One cannot say anything about the change in frequency of υ_4 for the Sc spinels since this band is only observed in the Raman spectrum of $CdSc_2S_4$. However, υ_4 is observed in all the Raman spectra of the *RE* spinels and there is a change of 16 and 15 cm^{-1} for the Yb and Tm spinels, respectively, when Mg is substituted for a Cd cation. The low-frequency mode υ_5 is only observed for the Cd–*RE* spinels and a comparison cannot be made. These must be two of the T_{2g} modes. Assignment of the T_{2g} modes to individual symmetry coordinates is not possible because of the necessity of forming linear combinations of symmetry coordinates belonging to the T_{2g} irreducible representation with coefficients which depend on the force constants.

υ_1 and υ_2 are not functions of the tetrahedral cation mass. Both are related to changes in the interatomic distances and unit cell volumes. This can be seen by plotting unit cell volume versus the υ_1 mode frequency (Fig. 5). In general, as the unit cell volumes and the interatomic distances increase through the series of compounds, υ_1 decreases in frequency. Because υ_1 and υ_2 depend mainly on interatomic distances and the interatomic forces and are independent of the tetrahedral cation masses, one must be the A_{1g} mode while the other must be the E_g mode. Examination of the symmetry coordinates for the A_{1g} and E_g modes in Table IV shows that the A_{1g} normal coordinate describes a stretching motion while the E_g normal coordinate describes a bending motion. Stretching modes generally have higher frequencies than bending modes. Tentatively, then, υ_2 is assigned as the E_g mode while υ_1 is assigned as the A_{1g} mode.

These assignments are in good agreement with the assignments obtained from single-crystal spectra of $CdIn_2S_4$ (*11*) and $CdCr_2S_4$ (*17*).

Assignment of the infrared modes to specific normal coordinates is more difficult because all five ir modes (including the zero-frequency acoustic mode) belonging to the T_{1u} represen-

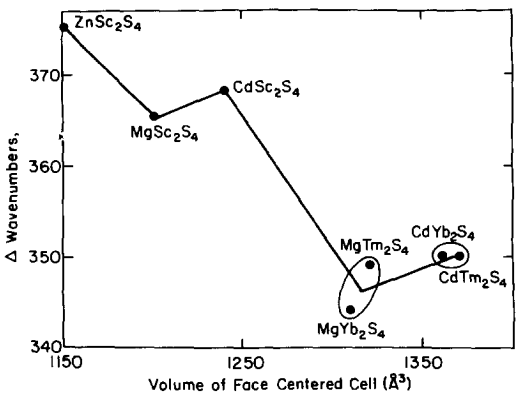

FIG. 5. Relation of υ_1 frequency to volume of spinel cell.

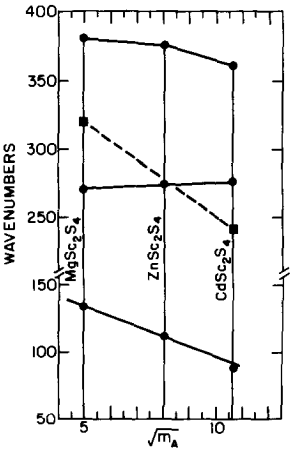

FIG. 6. Relation of the infrared-active modes to mass of the tetrahedral cation, m_A.

tation. The actual normal coordinates, when a model of the force field is included, will consist of linear combinations of symmetry coordinates. Some insight, however, can be obtained by examining the way in which the ir frequencies vary with spinel composition.

Figure 6 is a plot of mode frequency versus the square root of the mass of the A cation, $m_A^{1/2}$, for the four ir bands of the ASc_2S_4 compounds. Figure 6 demonstrates that two of the modes are independent of the tetrahedral cation mass while the other two bands are sensitive functions of the tetrahedral cation mass. The lowest-frequency band varies linearly with $m_A^{1/2}$. A similar observation has been made about the variation of the spectra of the Cd and Hg chromium selenide spinels (*10*). The weak band at 240 cm^{-1} in the $CdSc_2S_4$ spectrum shifts to 320 cm^{-1} in the $MgSc_2S_4$ spectrum but the band was not found in the $ZnSc_2S_4$ spectrum. The variation is marked with a dashed line, which suggests that this mode would directly overlap another band in $ZnSc_2S_4$, where only three ir bands are observed.

Next consider the infrared spectra of the ARE_2S_4 compounds, where A = Cd or Mg and RE = Yb or Tm. Only three of four fundamental modes occur consistently in all spectra. The weak band at 73 cm^{-1} in the Cd–RE spinels does not appear in the Mg–RE spinels. A comparison of band positions is given in Table V. Both the magnitudes and the directions of the shifts are identical even though the actual band positions are markedly different for these compounds.

Finally, consider the effect of changing the octahedral cation from Sc to an RE ion while keeping all the other ions the same. Table VI compares the frequencies of the four bands in the $CdTm_2S_4$ and $CdSc_2S_4$ spectra. There is a large change in the band position for the three higher bands, while the low-frequency band is insensitive to the octahedral cation mass. The low-frequency band shifts from 73 cm^{-1} in the $CdTm_2S_4$ spectrum to 89 cm^{-1} in the $CdSc_2S_4$ spectrum. Only a 16-cm^{-1} shift

TABLE V

COMPARISON OF INFRARED BAND SHIFTS FOR RE AND Sc SPINELS

	$CdTm_2S_4$	$MgTm_2S_4$	Δ	$CdSc_2S_4$	$MgSc_2S_4$	Δ
υ_8	151	232	81	240	320	80
υ_7	214	208	−6	275	270	−5
υ_6	300	320	20	361	380	19

TABLE VI

COMPARISON OF BAND POSITIONS IN THE SPECTRA OF $CdTm_2S_4$ AND $CdSc_2S_4$

	$CdTm_2S_4$	$CdSc_2S_4$	Δ
υ_9	73	89	16
υ_8	151	240	91
υ_7	214	275	61
υ_6	300	361	61

occurs even through Tm is 3.76 times more massive than Sc.

Some conclusions can now be drawn about the atomic motions which lead to the four bands found in the thiospinel spectra. υ_9 primarily involves movements of the tetrahedral cation while υ_6 and υ_7 are vibrations involving mainly the octahedral cations. υ_8, however, corresponds to a mode involving both the tetrahedral and octahedral cations as evidenced by its sensitivity to changes in both the octahedral and tetrahedral cation masses.

Force Constants for Sulfide Spinels

The force constant models that have been proposed for spinel compounds range in complexity from the *FG* matrix type, in which only nearest-neighbor interactions are included, to the lattice dynamic calculations, in which a rigid ion approximation with long-range coulombic forces are used. A model containing four force constants was previously used (*17*) to calculate the force constants and normal modes for $CdCr_2Se_4$ and $CdCr_2S_4$ with good success.

TABLE VII

FORCE CONSTANTS FOR THE SULFIDE SPINELS (mdyn/Å)[a]

Compound	f_1	f_2	f_3	f_4
$CdIn_2S_4$	1.03	0.0198	0.602	0.0342
$CdSc_2S_4$	1.41	0.029	0.607	0.036
$MgSc_2S_4$	0.738	−0.0066	0.573	0.105
$CdYb_2S_4$	0.938	0.042	0.562	0.041
$MgYb_2S_4$	0.516	0.055	0.335	0.122
$CdTm_2S_4$	0.948	0.040	0.582	0.042
$MgTm_2S_4$	0.495	0.059	0.380	0.120

[a] 1 mdyn/Å = 10^{-2} N/m.

The Brüesch and D'Ambrogio model consists of the following four force constants: a tetrahedral stretching force constant f_1, a tetrahedral angle bending force constant f_2, an octahedral stretching force constant f_3, and an octahedral angle bending force constant f_4. Because $u \simeq \frac{3}{8}$ for most sulfide spinels (Table I) this value was used to derive the dynamical equations. The equations are very simple and there is only one unique tetrahedral and octahedral angle for this value of the u parameter. See the original reference (*17*) for the specific form of the secular equations.

Force constants and normal coordinates were calculated for the sulfide spinels by an iterative procedure. The calculation was performed using the VA04A minimization subroutine (Harwell Subroutine Library) and the force constants were varied until observed and calculated frequencies agreed and the function

$$R = \sum_i \left[1 - \left(\frac{\upsilon_{i,\text{obs}}}{\upsilon_{i,\text{calc}}} \right)^2 \right]^2 \qquad (6)$$

was minimized, where i labels the data points.

Force constants and normal coordinates are listed in Tables VII and VIII. Nine modes were predicted from four force constants with an error no greater than 13%. In Table VIII both calculated and observed frequencies are listed along with the amplitudes of the symmetry coordinates that combine to form the normal coordinates. The normal coordinate Q_j corresponds to the mode frequency υ_j listed in Table III. T_x is one of the three degenerate acoustic normal coordinates. It was simplest to label the normal coordinates this way, rather than according to Eq. (5). The amplitudes are the $b^d(n,j)$ from Eq. (5) and are listed under the column labeled Normal Coordinates. The quantities S_{ji}^d are the symmetry coordinates listed in Table IV for the dth irreducible representations. While the b's are the amplitudes of the symmetry coordinates they are not the actual atomic amplitudes. The

atomic amplitude of atom k in the x, y, or z direction is obtained by dividing $b^d(n,j)$ by $m_k^{1/2}$ and multiplying the resulting quantity by the normalization constant of the symmetry coordinate S_{ji}^d and the weighting factor of the mass-weighted displacement coordinates x_k, y_k, or z_k in S_{ji}^d.

The bending is substantially stronger in the Sc compounds as opposed to the *RE* compounds for both Mg and Cd compounds. This is directly reflected by the substantially larger force constants in the Sc compounds. The comparison must be drawn between compounds with the same tetrahedral cation. On the other hand the stretching force constants for Cd compounds are always larger than the force constants for Mg compounds when the octahedral cation is kept constant. There is a larger change in the tetrahedral stretching force constant f_1 as opposed to the octahedral stretching force constant f_3 when a Cd ion is substituted for a Mg ion. This is particularly noticeable for the Sc and Tm spinels. This increase in the force constants for the Cd compounds occurs despite the fact that Mg is a smaller cation than Cd. One possible explanation is that Cd is more covalent and there is a short-range stabilization of the Cd ion in the structure compared with the more ionic Mg.

One cannot distinguish between internal (molecular type) and external modes for these sulfide spinels. The ir T_{1u} and the Raman-active T_{2g} normal coordinates are formed from a combination of all the symmetry coordinates in the respective irreducible representations and the weighting factors are of comparable magnitude. A distinction between internal and external modes can only be made for the spinel compounds if the tetrahedral bond strength is much greater than the octahedral bond strength, which Table VII indicates is not the case.

Intensity Calculations

Aside from comparing observed and calculated frequencies, one can test the Brüesch and D'Ambrogio model in yet another way. Observed and calculated absorption coefficients can be compared where the calculated values of the absorption are based on the force constant model.

The absorption of light which passes through a crystal is expressed as $\alpha(\upsilon)$, the absorption coefficient. If the absorption is a delta function, then there is only the possibility of a vibrational transition at the transverse mode frequency υ_j. While the above equality is not strictly true for real crystals in which the vibrations are damped it is often a good approximation. $\alpha(\upsilon_j)$ can be expressed as (*28*)

$$\alpha(\upsilon_j) = \frac{8\pi^3}{3ch}\,\upsilon_j |(\mu)_{0,j}|^2, \tag{7}$$

$$(\mu)_{0,j} = \langle \psi_0 | \mu | \psi_j \rangle. \tag{8}$$

The vertical brackets indicate that the magnitude of the vector is being taken. The dipole moment transition probability $(\mu)_{0,j}$ is from the ground state to the jth vibrational state. If only the jth mode is stimulated then the dipole moment can be expanded in terms of its normal coordinate Q_j. Thus

$$\mu(Q_j) = \mu_0 + \left(\frac{d\mu}{dQ_j}\right)_0 Q_j + \left(\frac{d^2\mu}{dQ_j^2}\right)_0 Q_j^2 + \cdots. \tag{9}$$

If we only use the linear terms in the expansion we obtain the following for the square of the magnitude of the transition moment probability:

$$|(\mu(Q_j))_{0,j}|^2 = \left| \langle \psi_0 | \left(\frac{d\mu}{dQ_j}\right)_{\text{equil}} Q_j | \psi_j \rangle \right|^2$$

$$= \left| \left(\frac{d\mu}{dQ_j}\right)_{\text{equil}} \right|^2 \langle \psi_0 | Q_j | \psi_j \rangle^2$$

$$= \frac{h}{4\pi^2 \omega_j} \left| \left(\frac{d\mu}{dQ_j}\right)_{\text{equil}} \right|^2. \tag{10}$$

The induced dipole moment in terms of mass-weighted displacement coordinates is given as

$$\mu = \sum_{k\alpha} \frac{c_k}{m_k^{1/2}}\, x_{k\alpha}. \tag{11}$$

TABLE VIII

NORMAL COORDINATES FOR THE SULFIDE SPINELS AND A COMPARISON BETWEEN OBSERVED AND CALCULATED FREQUENCIES

		Frequencies		Normal coordinates					
d	Compound	Obs	Calc	Label	S_{11}^d	S_{21}^d	S_{31}^d	S_{41}^d	S_{51}^d
A_{1g}	$CdIn_2S_4$	362	317	Q_1	1.0				
	$CdTm_2S_4$	350	314		1.0				
	$MgTm_2S_4$	349	312		1.0				
	$CdYb_2S_4$	350	311		1.0				
	$MgYb_2S_4$	344	311		1.0				
	$CdSc_2S_4$	368	350		1.0				
	$MgSc_2S_4$	365	338		1.0				
E_g	$CdIn_2S_4$	184	197	Q_2	1.0				
	$CdTm_2S_4$	215	204		1.0				
	$MgTm_2S_4$	217	205		1.0				
	$CdYb_2S_4$	204	202		1.0				
	$MgYb_2S_4$	202	199		1.0				
	$CdSc_2S_4$	218	202		1.0				
	$MgSc_2S_4$	216	201		1.0				
T_{2g}	$CdIn_2S_4$	93	92	Q_5	0.923	0.281	0.264		
		242	218	Q_4	−0.0873	0.819	−0.566		
		307	324	Q_3	−0.375	0.499	0.781		
	$CdTm_2S_4$	95	96	Q_5	0.920	0.313	0.236		
		259	227	Q_4	−0.129	0.811	−0.570		
		—	315	Q_3	−0.370	0.494	0.787		
	$MgTm_2S_4$	—	158	Q_5	0.645	0.668	0.372		
		274	181	Q_4	−0.211	0.623	−0.753		
		—	317	Q_3	−0.735	0.407	0.543		
	$CdYb_2S_4$	96	95.8	Q_5	0.918	0.320	0.235		
		251	225	Q_4	−0.135	0.808	−0.574		
		—	313	Q_3	−0.373	0.495	0.785		
	$MgYb_2S_4$	—	153	Q_5	0.638	0.669	0.381		
		267	277	Q_4	−0.225	0.636	−0.738		
		—	319	Q_3	−0.736	0.385	0.557		
	$CdSc_2S_4$	99	98	Q_5	0.906	0.319	0.279		
		265	223	Q_4	−0.101	0.803	−0.588		
		—	365	Q_3	−0.411	0.504	0.759		

	$MgSc_2S_4$	155	148	Q_5	0.754	**0.471**	**0.459**		
		—	265	Q_4	−0.190	**0.824**	**−0.535**		
		—	359	Q_3	−0.630	**0.316**	**0.710**		
T_{1u}	$CdIn_2S_4$	68	70	Q_9	−0.524	0.256	0.650	0.149	−0.463
		170	148	Q_8	0.612	−0.430	0.664	0.00183	0.00348
		231	246	Q_7	0.00695	−0.480	−0.316	0.635	−0.514
		311	336	Q_6	−0.334	−0.176	0.188	0.548	0.722
		0	0	T_x	0.489	0.698	0	0.523	0
	$CdTm_2S_4$	73	75	Q_9	−0.437	0.204	0.782	0.0784	−0.387
		151	134	Q_8	0.706	−0.440	0.546	0.0532	0.0849
		214	237	Q_7	−0.0291	−0.398	−0.260	0.673	−0.566
		300	325	Q_6	−0.340	−0.151	0.151	0.563	0.723
		0	0	T_x	0.441	0.764	0	0.471	0
	$MgTm_2S_4$	—	117	Q_9	−0.107	0.0267	0.954	0.00340	−0.276
		208	203	Q_7	0.712	−0.407	0.206	0.350	0.403
		232	249	Q_8	0.0180	−0.338	−0.205	0.542	−0.741
		320	330	Q_6	−0.656	−0.174	0.0623	0.568	0.461
		0	0	T_x	0.223	0.830	0	0.511	0
	$CdYb_2S_4$	72.5	74.7	Q_9	−0.425	0.198	0.794	0.0732	−0.380
		152	132	Q_8	0.712	−0.443	0.532	0.0613	0.0950
		214	233	Q_7	−0.0344	−0.391	−0.256	0.675	−0.570
		295	323	Q_6	−0.344	−0.147	0.145	0.563	0.722
		0	0	T_x	0.438	0.768	0	0.468	0
	$MgYb_2S_4$	—	115	Q_9	−0.106	0.0262	0.961	0.00282	−0.254
		211	198	Q_7	0.701	−0.397	0.202	0.347	0.435
		230	243	Q_8	0.0195	−0.351	−0.181	0.568	−0.722
		320	331	Q_6	−0.669	−0.156	0.0548	0.547	0.474
		0	0	T_x	0.221	0.833	0	0.507	0
	$CdSc_2S_4$	89	92	Q_9	−0.555	0.281	0.453	0.285	−0.572
		240	219	Q_8	0.490	−0.449	0.723	−0.0834	−0.167
		275	308	Q_7	0.0288	−0.612	−0.445	0.485	−0.438
		361	389	Q_6	−0.331	−0.271	0.274	0.537	0.673
		0	0	T_x	0.583	0.522	0	0.623	0
	$MgSc_2S_4$	133	135	Q_9	−0.545	0.136	0.439	0.123	−0.691
		270	268	Q_7	0.603	−0.295	0.738	−0.0158	−0.0688
		320	341	Q_8	0.237	−0.565	−0.461	0.370	0.525
		380	393	Q_6	0.427	−0.452	0.227	0.564	0.493
		0	0	T_x	0.316	0.609	0	0.727	0

The transformation from mass-weighted displacement coordinates to normal coordinates is given by

$$x_{k\alpha} = \sum_{j=1}^{3N} e(k\alpha, j|0)Q_j, \quad (12)$$

$$u = \sum_{k\alpha} \sum_{j} \frac{c_k}{m_k^{1/2}} e(k\alpha, j|0)Q_j, \quad (13)$$

$$\frac{d\mu}{dQ_j} = \sum_{k,\alpha} \sum_{j} \frac{c_k}{m_k^{1/2}} e(k\alpha, j|0), \quad (14)$$

$$\alpha(\upsilon_j) = \frac{2\pi}{3c} \left| \sum_{k\alpha} \frac{c_k}{m_k^{1/2}} e(k, \alpha, j|0) \right|^2 \quad (15)$$

Thus if we know the electrostatic charge c_k on atom k and the vibrational amplitude of atom k in the α direction in the jth normal mode we can calculate the absorption $\alpha(\upsilon_j)$.

Using Eq. (15) it is now possible to calculate the absorption by a particular mode using the calculated normal coordinates of the Brüesch and D'Ambrogio model. This was done for $CdIn_2S_4$, where the calculated values could be checked against the experimental values for the four ir modes (Table IX). Because the absorption coefficient contains constants and a scaling parameter which scales the ionic charges (the scaling parameter is used to maintain charge neutrality and because the absolute charges on the individual ions are not known), the results are presented in the form of relative absorptions, $\alpha_{rel}(\upsilon_j)$. Note that Eq. (15) yields zero intensities for all the Raman modes and the acoustic modes as it must.

Calculated relative absorbance intensities for the spinels examined in this study are given in Table X. The results of the calculation

TABLE IX

CALCULATED AND OBSERVED RELATIVE ABSORPTIONS OF THE INFRARED BANDS OF $CdIn_2S_4$

υ_j	$\alpha_{rel}^{obs}(\upsilon_j)$	$\alpha_{rel}^{calc}(\upsilon_j)$
68	0.0108	0.0255
171	0.0830	0.00773
215	1.00	1.00
307	0.529	0.664

TABLE X

CALCULATED VALUES FOR THE RELATIVE ABSORPTIONS FOR SULFIDE SPINELS

Compound	$\alpha_{rel}(\upsilon_6)$	$\alpha_{rel}(\upsilon_7)$	$\alpha_{rel}(\upsilon_8)$	$\alpha_{rel}(\upsilon_9)$
$CdTm_2S_4$	0.702	1.00	0.0061	0.014
$CdYb_2S_4$	0.700	1.00	0.0072	0.012
$CdSc_2S_4$	0.720	1.00	0.034	0.031
$MgTm_2S_4$	1.00	0.016	0.448	0.0027
$MgYb_2S_4$	1.00	0.016	0.512	0.0059
$MgSc_2S_4$	1.00	0.0065	0.371	0.066

indicate that for the Cd spinels there should be two very intense ir bands at high frequencies and two rather weak ir bands at low frequencies. The qualitative agreement with the observed powder spectra is good. The agreement for the Mg spinels is less satisfactory, perhaps partly because of overlapping bands, which violates an assumption made in deriving Eq. (15). Thus the model uses four force constants to predict with reasonable precision not only the frequencies of nine modes, but also the intensities of the four ir modes.

Acknowledgments

We are grateful to Professor J. M. Pliva and Dr. S. A. Brawer for many helpful discussions of the force constant calculations. C. A. Smith is thanked for her aid in the unit cell refinements.

References

1. J. PREUDHOMME AND P. TARTE, *Spectrochim. Acta A* **27**, 961 (1971).
2. J. PREUDHOMME AND P. TARTE, *Spectrochim. Acta A* **27**, 845 (1971).
3. J. PREUDHOMME AND P. TARTE, *Spectrochim. Acta A* **27**, 1817 (1971).
4. J. PREUDHOMME AND P. TARTE, *Spectrochim. Acta A* **28**, 69 (1972).
5. H. D. LUTZ AND M. FEHER, *Spectrochim. Acta A* **27**, 357 (1971).
6. K. YAMAMOTO, T. MURAKAWA, Y. OBAYASHI, H. SHIMIZU, AND K. ABE, *J. Phys. Soc. Japan* **35**, 1258 (1973).
7. H. SHIMIZU, Y. OHBAYASHI, K. YAMAMOTO, AND K. ABE, *J. Phys. Soc. Japan* **38**, 750 (1975).

8. T. ARAI, K. WAKAMURA, AND K. KUDO, *J. Phys. Soc. Japan* **30**, 1762 (1971).
9. V. WAGNER, H. MITLEHNER, AND R. GEICK, *Opt. Commun.* **2**, 429 (1971).
10. K. WAKAMURA, S. ONARI, T. ARAI, AND K. KUDO, *J. Phys. Soc. Japan* **31**, 1845 (1971).
11. H. VAN DEN BOOM AND J. H. HAANSTRA, *J. Raman Spectrosc.* **2**, 265 (1974).
12. N. KOSHIZUKA, Y. YOKOYAMA, H. HIRUMA, AND T. TSUSHIMA, *Solid State Commun.* **16**, 1011 (1975).
13. E. F. STEIGMEIER AND G. HARBEKE, *Phys. Kondens. Mater.* **12**, 1 (1970).
14. W. B. WHITE AND B. A. DEANGELIS, *Spectrochim. Acta A* **23**, 985 (1967).
15. R. D. WALDRON, *Phys. Rev.* **99**, 1727 (1955).
16. B. A. DEANGELIS, Ph.D. Dissertation, The Pennsylvania State University (1969).
17. P. BRÜESCH AND F. D'AMBROGIO, *Phys. Status Solidi B* **50**, 513 (1972).
18. H. D. LUTZ AND H. HAEUSELER, *Ber. Bunsenges. Phys. Chem.* **79**, 605 (1975).
19. M. E. STRIEFLER AND G. R. BARSCH, *J. Phys. Chem. Solids* **33**, 2229 (1972).
20. W. M. YIM, A. K. FAN, AND E. J. STOFKO, *J. Electrochem. Soc.* **120**, 441 (1973).
21. M. PATRIE, J. FLAHOUT, AND L. DOMANGE, *C. R. Acad. Sci.* **258**, 2585 (1964).
22. L. SUCHOW AND N. STEMPLE, *J. Electrochem. Soc.* **111**, 191 (1964).
23. R. C. C. LEITE AND S. P. S. PORTO, *Phys. Rev. Lett.* **17**, 10 (1966).
24. M. BORN AND K. HUANG, "Dynamical Theory of Crystal Lattices," Oxford Univ. Press (Clarendon), London(1962).
25. T. SHIMANOUCHI, T. MASAMICHI, AND T. MIYAZAWA, *J. Chem. Phys.* **35**, (1957).
26. T. G. WORLTON AND J. L. WARREN, *Comp. Phys. Commun.* **3**, 88 (1972).
27. F. A. COTTON, "Chemical Applications of Group Theory," 2nd ed., Wiley–Interscience, New York, (1971).
28. E. B. WILSON, JR., J. C. DECIUS, AND P. C. CROSS, "Molecular Vibrations" McGraw-Hill, New York (1955).
29. M. P. O'HORO, A. L. FRISILLO, AND W. B. WHITE, *J. Phys. Chem. Solids* **34**, 23 (1973).